



저작자표시-비영리-변경금지 2.0 대한민국

이용자는 아래의 조건을 따르는 경우에 한하여 자유롭게

- 이 저작물을 복제, 배포, 전송, 전시, 공연 및 방송할 수 있습니다.

다음과 같은 조건을 따라야 합니다:



저작자표시. 귀하는 원저작자를 표시하여야 합니다.



비영리. 귀하는 이 저작물을 영리 목적으로 이용할 수 없습니다.



변경금지. 귀하는 이 저작물을 개작, 변형 또는 가공할 수 없습니다.

- 귀하는, 이 저작물의 재이용이나 배포의 경우, 이 저작물에 적용된 이용허락조건을 명확하게 나타내어야 합니다.
- 저작권자로부터 별도의 허가를 받으면 이러한 조건들은 적용되지 않습니다.

저작권법에 따른 이용자의 권리는 위의 내용에 의하여 영향을 받지 않습니다.

이것은 [이용허락규약\(Legal Code\)](#)을 이해하기 쉽게 요약한 것입니다.

[Disclaimer](#)

이학석사학위논문

**SOD1 돌연변이에 의한 신경세포와
성상아교세포에서의 세포질 이상응집
현상에 관한 연구**

An examination of mutant
superoxide dismutase-1 in
modulating the mislocalization and
aggregation of ALS-associated
SOD1 in neurons and astrocytes

2014 년 8 월

서울대학교 대학원
뇌 과학 협 동 과 정
이 도 연

**SOD1 돌연변이에 의한 신경세포와
성상아교세포에서의 세포질 이상응집
현상에 관한 연구**

An examination of mutant
superoxide dismutase-1 in
modulating the mislocalization and
aggregation of ALS-associated
SOD1 in neurons and astrocytes

지도교수 이 광 우

이 논문을 이학석사학위논문으로 제출함

2014 년 8 월

서울대학교 대학원

뇌 과 학 협 동 과 정

이 도 연

이도연의 석사학위논문을 인준함

2014 년 8 월

위원장_____ (인)

부위원장_____ (인)

부위원장_____ (인)

**An examination of mutant superoxide
dismutase-1 in modulating the
mislocalization and aggregation of ALS-
associated SOD1 in neurons and
astrocytes**

by

Do-yeon Lee

A Thesis Submitted in Fulfillment of the Requirements for

The Degree of Master of Science

in Seoul National University, Seoul, Korea

August 2014

Professor Chairman

Professor Vice chairman

Professor

Abstract

Mutations in superoxide dismutase-1 (SOD1) are associated with familial cases of amyotrophic lateral sclerosis (fALS). Owing to the similarities in sporadic and fALS forms, mutant SOD1 animal and cellular models are a useful tool to study the disease. In transgenic mice expressing either wild-type (wt) human SOD1 or mutant G93A-SOD1, we found that wtSOD1 was present in cytoplasm and in nuclei of cortical neurons and astrocytes, whereas mutant SOD1 was mainly cytoplasmic. Furthermore, mutant-type SOD1 can modulate the form of wtSOD1 in cortical neurons and astrocytes by transfection. Cells expressing G93A-SOD1 showed a higher DNA damage compared with those expressing wtSOD1, possibly because of a loss of nuclear protection. We show that mutant G93A-SOD1 modulates the mislocalization and aggregation in ALS-associated SOD1 in cortical neurons and astrocytes that through wtSOD1 transformed mutant form by transfected with G93A-SOD1. These findings implicate that soluble assembly of wt and mtSOD1 as possible mediators of toxic processes involved in initiating mislocalization and aggregation. Here, we provide evidence that cytoplasmic aggregates induce apoptosis in G93A-SOD1 mouse cortical neurons and astrocytes. Taken together, our results indicate that mtSOD1 is probably interacting with wtSOD1 via some mechanisms to produce the augmented toxicity and may influence the formation of aggregates and apoptosis.

Key words: amyotrophic lateral sclerosis, cortical astrocyte, cortical neuron, G93A SOD1, mislocalization, apoptosis

Student Number: 2012-20408

Contents

Abstract	2
Contents	4
List of Figures	5
Introduction	6
Materials and Methods	12
Results	19
Discussion	40
References	45
국문초록	53

List of Figures

Fig. 1 Cellular and morphological characterization of astrocyte and neuron enriched cultures -----	24
Fig. 2 WT neuronal cells transformed mutant form by transfection G93A-SOD1-----	26
Fig. 3 WT neuronal cells transformed mutant form by transfection G93A-SOD1 -----	28
Fig. 4 WT and mutant astrocytes transformed mutant form by transfection GFP-wild type and G93A-SOD1 -----	30
Fig. 5 Cytoplasmic mislocalization of SOD1 in the wild-type and mutant astrocytes by transfection GFP-wild type and G93A-SOD1---	32
Fig. 6 Aggregated formation of mutant SOD1 in mutated astrocytes by transfection GFP-mutant SOD1 -----	34
Fig. 7 Expression of both wt-SOD1 and mt-SOD1 induces cell death by transfection mutant SOD1 in astrocytes -----	36
Fig. 8 Cytoplasmic accumulation of protein aggregates in primary astrocytes promote apoptosis -----	38

I . Introduction

Amyotrophic lateral sclerosis (ALS) results from progressive loss of upper and lower motor neurons and denervation atrophy of skeletal muscles (Lim et al., 2012). Progressive muscle denervation leads to spreading failure of the neuromuscular system resulting in death in most cases from respiratory failure within 2-3 years of symptom onset (Beghi et al., 2007). Most of the cases are sporadic (sALS), but 10% are familial (fALS) forms inherited in a dominant manner and about 20% of these are linked to mutations of Cu/Zn superoxide dismutase type-1 (SOD1), a crucial enzyme for cellular antioxidant defense mechanisms (Rosen et al., 1993). As sALS and SOD1-mediated fALS are clinically indistinguishable and both affect motoneurons with a similar pathology, mutant SOD1 animal and cellular models represent a useful tool to study the disease (Bendotti et al., 2004). SOD1 normally functions in the regulation of oxidative stress by conversion of free radical superoxide anions to hydrogen peroxide and molecular oxygen (Morris, et al 1998). In 1993 the first causative mutations were found within the gene encoding the enzyme, superoxide dismutase 1 (SOD1) (Deng et al., 1993; Rosen et al., 1993). Since then, over 155 SOD1 mutations have been described (although pathogenicity has not been shown for all of these changes) and these mutations account for up to 20 % of familial ALS cases and 3 % of sporadic ALS cases (Pasinelli and Brown, 2006; Acevedo-Arozena et al., 2011; Andersen and Al Chalabi, 2011).

SOD1 is ubiquitously expressed and highly conserved across species (Fridovich, 1995). The gene is composed of five exons encoding a 153 amino acid metalloenzyme, also referred to as Cu/Zn superoxide dismutase. Most mutations are point substitutions but a few produce truncated proteins due to early termination. The protein localizes to the cytoplasm, nucleus, lysosomes and intermembrane space of mitochondria (Chang et al., 1988; Keller et al., 1991; Crapo et al., 1992; Sturtz et al., 2001). It binds copper and zinc ions and forms a homodimer whose main known function is as a dismutase removing dangerous superoxide radicals by metabolizing them to molecular oxygen and hydrogen peroxide, thus providing a defence against oxygen toxicity (Reddi and Culotta, 2013). Further, SOD1 is produced at high levels that have not yet been explained by known functions, therefore, it may well play other roles both neuron-specific and generally (Reddi and Culotta, 2013).

The finding of loss of dismutase activity in patients with ALS and the distribution of ALS-causative mutations spread throughout the SOD1 gene initially suggested loss of function as a mechanism (Deng et al., 1993; Rosen et al., 1993). Transgenic mice overexpressing human SOD1 with a glycine to alanine mutation in position 93 (Tg G93A-SOD1 mice) develop an ALS-like phenotype, even in the presence of the endogenous enzyme (Gurney et al., 1994), whereas SOD1 knockout mice do not develop ALS, despite the toxicity of the superoxide radicals (Shefner et al., 1999). However, the exact nature of the toxicity and of the causes of the motoneuronal degeneration is still largely debated (Pasinelli and

Brown, 2006).

The disease-associated mutations are known to destabilize the protein, and compelling data support the notion that fALS should be considered a protein misfolding disorder, in which a non-native toxic oligomeric conformation is generated in the mutant proteins (Pasinelli and Brown, 2006). Protein misfolding may subsequently trigger a cascade of events which included protein accumulation, possibly followed by axonal transport alteration, mitochondrial and/or proteasome dysfunctions. Moreover, these events may indirectly lead to overproduction of reactive oxygen species (ROS) and caspase activation (Bendotti and Carri, 2004).

ALS-associated mutations in SOD1, both missense and premature termination, include misfolding and aggregation of the protein (Wang et al 2003). In studies of G93A transgenic mice that model SOD1-fALS, sedimentable detergent-insoluble aggregates of mutant SOD1 first begin to accumulate at approximately the time that symptoms become first noticeable (at ~ 80 days of age) (Basso, 2006). Both theoretical models (Wang et al., 2008) and cell culture models (Prudencio et al., 2009) have produced data to suggest that mutations imparting a high propensity to aggregate are disproportionately associated with disease of shorter duration. Thus, we have proposed that large aggregates may modulate the rate of disease progression in humans with forms of mutant SOD1 that are soluble being responsible for initiating disease (Prudencio et al., 2009).

The molecular features of the mutant SOD1 responsible for initiating

disease have yet to be defined. Recent studies have focused our attention on the possible role of WT SOD1 as a modulator of disease initiation. In mice that express mutants in which the mutant protein is easily distinguished from WT SOD1, such as the G85R, T116X and L126Z mutants, it has been possible to determine that earlier disease onset is accompanied by the formation of detergent-insoluble aggregates that appear to contain both WT hSOD1 and mutant hSOD1 (Deng et al., 2006). *In vitro*, small amounts of immature mutant SOD1 can seed the aggregation of WT SOD1 (Chattopadhyay et al., 2008). Collectively, these studies indicate a potential for WT hSOD1 to play a role in the aggregation of mutant SOD1 and to modulate the course of disease.

More recently, Deng et al. (2006), using double transgenic mice overexpress also existing both wt and mutant human SOD1, demonstrated that human wtSOD1 is able to exacerbate the ALS-like disease progression and to form aggregates, thus suggesting that the conversion into an insoluble status, that segregates the active enzyme, may be sufficient to induce the pathological conditions. This may explain why in our study the mutant SOD1 transfected into the WT cells were affected by the the mutant G93A-SOD1. Interestingly, in our experiments the expression of mutant SOD1 correlates with a transform of the endogenous SOD1, and this may also explain the reduced protection from the oxidative damage at the DNA level. Several data are indeed accumulating showing that the levels of oxidative damage to DNA are increased in sALS patients (Fitzmaurice et al., 1996) and in an animal model of ALS (Aguirre et al., 2005). Moreover, the existence of nuclear

aggregates in motoneurons of an ALS patient has also been recently reported (Seilhean et al., 2004).

On the basis of our results, showing that G93A-SOD1 is excluded from the nucleus, the effect we have observed could be at least in part ascribed to the increased concentration of aggregates in the both nucleus and cytoplasm in astrocytes and neuronal cells. We have used cell models to examine interactions between WT and mutant hSOD1 in aggregate formation. It remains to be determined whether the altered transfected distribution of G93A-SOD1 may be increase SOD1 aggregation. Therefore, SOD1 aggregation may lead to alteration of the redox system itself, thus amplifying the mutant SOD1-mediated toxicity (Kondo, et al 1997).

Oxidative impairment of mitochondrial function causes bioenergetics failure through the activation of different mechanisms and production of oxidative molecules, leading to subsequent cell death and brain damage (Sofroniew and Vinters, 2010). Mitochondrial protection in astrocytes is fundamental for maintaining the energetic balance of the brain and antioxidant production that contributes to neuronal protection (Dugan and Kim-Han, 2004; Greenamyre et al., 2003).

Here we provided what is known about SOD1 loss of function and the evidence to suggest it may play a role in ALS pathogenesis after all, possibly through increased susceptibility to neurodegeneration. In addition, mitochondria in G93A-SOD1 expressing astrocytes display severe impairment of nucleus damage. Mitochondrial dysfunction results

in decreased ability to sustain motor neuron survival. Together, our results suggest that mitochondrial activity in astrocytes greatly influences their subsequent ability to regulate motor neuron survival. SOD1 loss has effect on both neuronal and non-nervous system cells. In the present study, we compared the phenotype of cultured astrocytes and neurons derived from the cortex of wild-type and human SOD1 gene (human G93A-SOD1) mice embryos, and confirmed the expression of aggregation in cells obtained from the mutant SOD1 by transfection.

II. Materials and methods

Identification of transgenic mouse embryos expressing hSOD1^{G93A}

Transgenic mice originally obtained from Jackson Laboratories (Bar Harbor, ME) and expressing high copy number of mutant human SOD1 with Gly93Ala substitution (TgSOD1 G93A) were bred and maintained on a B6/SJL mice strain. The animals were housed in standard conditions: constant temperature ($22 \pm 1^\circ\text{C}$), humidity (relative, 40%), and a 12-h light/dark cycle and were allowed free access to food and water. Genomic DNA was extracted from a mouse embryo tail biopsy obtained. Some 500ng genomic DNA was subjected to PCR using specific primers for hSOD1^{wt}: (forward) 5'-CTAGGCCACAGAATTGAAAGATCT-3' (reverse) 5'-GTAGGTGGAAATTCTAGCATCATCC-3' and hSOD1^{G93A}: (forward) 5'-CATCAGCCCTAATCCATCTGA-3' (reverse) 5'-CGCGACTAACAATCAAA GTGA-3'; the programme consisted of 35 cycles of denaturation (98°C for 10s), annealing (64°C for 40s) and extension (72°C for 1min). A $10\mu\text{l}$ aliquot of each sample was electrophoresed on an 1.2% agarose gel. The experiments were performed in accordance with local and international regulations, every effort was made to reduce the number of animals used and to minimize their suffering. For all studies, control primary cultures were obtained from littermates negative for the transgene to insure the use of an appropriate control.

Antibodies and reagents

Antibodies against beta-actin (1:2,000, Santa Cruz), cleaved caspase-3 (1:1,000), GFP (1:2,000, RockLand), glial fibrillary acidic protein (GFAP; 1:500, Sigma), and Map2a,b,c-3 (1:500, NeoMarkers) were used in study. The primary astrocytes cultured in Dulbecco's modified Eagle's medium (DMEM; WELGENE) supplemented with 10 % fetal bovine serum (Gibco), 100 U/mL penicillin, and 0.1 mg/mL streptomycin (Gibco). The primary neuronal cell cultured in neurobasal (Gibco) supplemented with 2mM L-Glutamine (Gibco), 2% B-27 (Invitrogen). All cells were maintained in a humidified atmosphere containing 5% CO₂ at 37 °C.

Primary cortical astrocyte cultures

Primary cortical astrocyte cultures were prepared from the cortex of 15-16-day old mouse embryos. Briefly, cortices were dissected away from embryos (neonatal day 15-16) and the meninges were removed and incubated in activated papain solution in Ca²⁺- and Mg²⁺- free Hank's balanced salt solution (HBSS) (Gibco) for 15min at 37°C, digested by incubation with 2/5 V/V trypsin for 15min at 37°C. Purified tissues were triturated by repeated pipetting with blue tip and yellow tip to ensure full dissociation into single cells. The cells were washed with complete medium (Dulbecco's Modified Eagle's Medium (DMEM); Welgene) supplemented with 10% fetal bovine serum (Gibco), 100µg/mL

streptomycin, 100U/mL penicillin (Gibco) once and centrifuged at 1,000rpm for 5min. The supernatant was removed and the pellet was resuspended in complete medium. The cells were plated onto 60mm dishes. The cells were allowed to proliferate until confluence was achieved. At this point, arabinofuranosylcytidine (AraC, 10 μ M, Sigma) was added to avoid the growth of oligodendrocytes. These cultures were maintained in complete medium. Cells were cultured at 37°C in a humidified atmosphere of 95% air and 5% CO₂. Cells were used for transfection after 15-16 days *in vitro* when the astrocytes were confluent and neither neurons nor oligodendrocytes could be found in cultures. Astrocytes cultures from this passage (P1) were used for all studies.

Primary cortical neuronal Culture

Cortical neuronal cultures were prepared from the cortex of 15-16-day old mouse embryos. Briefly, cortices were dissected away from embryos (neonatal day 15-16) and the meninges were removed and incubated in activated papain solution in Ca²⁺ - and Mg²⁺- free Hank's balanced salt solution (HBSS) (Gibco) for 15min at 37°C, digested by incubation with 2/5 V/V trypsin for 15min at 37°C. Purified tissues were triturated by repeated pipetting with blue tip and yellow tip to ensure full dissociation into single cells. The cells were washed with complete medium (Gibco) supplemented with 2mM L-Glutamine (Gibco) , 2% B-27 (Invitrogen) once and centrifuged at 1,000rpm for 5min. The supernatant was removed and the pellet was resuspended in complete medium. The cells

were plated on glass coverslips onto 6-well plates. All plates were precoated with 50µg/ml poly-d-lysine (Sigma) and grown in neurobasal medium (Invitrogen) supplemented with B27 and 2mM glutamine (Invitrogen). In B27/neurobasal medium, glial growth was reduced to less than 0.5%. The vast majority of cultured cells were immunoreactive for neuron-specific enolase. The cultures were incubated at 37°C in 95% air/5% carbon dioxide with 95% humidity. Neuron-conditioned medium was changed every 2 days during the maturation of cortical neurons. Cultures were used for experiments on the 10th day *in vitro* (DIV 10).

Cell transfection with human SOD1 gene

Primary cortical astrocyte cultures were transfected after 15-16 days *in vitro* using LipofectAMINE2000 reagent (Invitrogen), following the manufacturer's protocol. The transfection was performed in a 10% FBS medium and without antibiotics. Cultured astrocytes treated with the pcN1 vector only were used as negative controls. Transfection efficiency was tested by using the vector containing a Green Fluorescent Protein (GFP) gene.

Protein extraction and western blot analysis

Total proteins from the transfected cells were extracted with RIPA buffer (25mM Tris-HCl (pH 7.4), 5mM EDTA, and 137mM NaCl, 1 % Triton X-100,

1 % Sodium deoxycholate, 0.1 % SDS) containing protease inhibitor cocktail tablets (Roche, Mannheim, Germany). Protein concentrations were determined using the BCA assay, using bovine serum albumin as a standard. Cell lysates were centrifuged at 12,000g for 10 min at 4°C and supernatant was transferred to e-tube. Samples were boiled in sample loading buffer at 100°C for 10 min, separated on 10% SDS-polyacrylamide gel, and transferred to a nitrocellulose membranes. The membranes was incubated with 5% skim milk in TBS-T (50mM Tris, 200mM NaCl, 0.05% Tween20, pH 7.5) for 1 hr to block nonspecific protein binding. After washing three times for 10 min with 0.1% TBS-T, the membranes were then incubated with primary antibodies. As a control for protein loading, blots were subsequently probed for mouse anti β -actin (1:1,000: Cell signaling, Beverly, MA, USA) using the same procedures. After washing three times for 10 min with 0.1% TBS-T, immunoreactive antibodies were further incubated with appropriated secondary antibodies conjugated to horseradish peroxidase in 5% skim milk in TBS-T, the membranes were detected by SuperSignal West Substrate (Pierce) and exposed to Chemifluorescence. Data were calculated as the ratio of mean target gene intensity to β -actin intensity. Densitometric analysis of Western blots was performed using J-image software to measure the area and density of protein bands.

Immunocytochemistry and immunofluorescence studies

Cells were plated on poly-D-Lysine (mw 70-150,000, Sigma) coated 24-well plates or 6-well plates (SPL). For immunocytochemistry studies, astrocytes and neuronal cells (24-48 hr after transfection) were fixed with 4% paraformaldehyde (PFA) for 15 min at room temperature and then washed three times in PBS, permeabilized with 0.5% Triton X-100 for 5 min, and washed three times. Nonspecific antibody binding was minimized by incubation in blocking solution (5% bovine serum albumin in 0.3% PBS-T) for 30 min at RT. Cells were incubated with primary antibodies to mouse anti-GFAP (1:500) or mouse anti-Map2 (1:500) for 12h at 4°C. After washing, the cells were incubated anti-mouse secondary antibody conjugated with Alexa 555 (1:200, Invitrogen) for 1h at RT. Nuclear DNA was stained by 4,6-diamino-2-phenylindole (DAPI; 1:1,000, sigma) and allow assessment of nuclear morphology to determine apoptosis. And, following rinsing twice with PBS, the coverslips were mounted on glass slide using Dako Fluorescent mounting medium (Dako). Cells were visualized using a fluorescence microscope (Leica) coupled to a digital camera.

Quantitative real-time (qRT-) PCR

Total RNA was extracted from astrocytes by TRIzol reagent (MRC, Cincinnati, OH, USA). RNA (50 ng) were used as a template for qRT-PCR amplification, using SYBR green real-time PCR master mix (Toyobo, Osaka, Japan). Primers were standardized in the linear range of the cycle before the onset of the plateau. GAPDH was used as an internal control.

Two-step PCR thermal cycling for DNA amplification and real-time data acquisition were performed with an ABI 7500 real-time PCR system.

III. Results

Cellular and morphological characterization of astrocyte and neuron enriched cultures

Astrocyte and neuron enriched primary cultures were generated from neonatal 16 days mutant G93A-SOD1 mice embryos. The use of appropriate culture medium combined with a vigorous chemical and mechanical dissociation step promoted the enrichment of astrocytes and neurons and the elimination of oligodendrocytes from the culture. To evaluate the purity of our cultures we employed an extensive marker analysis and found high levels of well-known astrocyte and neuronal markers including GFAP and Map2a,b,c -3 (Fig. 1A). The cultures obtained from transgenic mice embryos were morphologically indistinguishable from control cultures. Prior to activation, both wild-type and transgenic astrocyte and neuron cultures maintained a polygonal flat morphology. Western blot analysis confirmed the presence of the human SOD1 in cortical neurons and astrocytes (Fig. 1B).

Wild-type astrocyte and neuronal cells transformed mutant form by transfection G93A-SOD1

In this study, we have transfected cortical neurons and astrocytes with

plasmids encoding either the wtSOD1 or the G93A-SOD1, subsequently detected by immunocytochemistry. The results show that in most of the cortical neurons and astrocytes transfected with G93A-SOD1, the immunoreactivity for SOD1 is mainly diffusely mislocalized in nucleus. In addition, supporting the evidence that the nuclear fluorescence observed in Fig. 2 and Fig. 4 is due to the nuclear localization of wtSOD1. Immunocytochemistry was performed on paraformaldehyde-fixed cells grown on glass coverslips from mice embryonic cortices using GFAP, Map2a,b,c-3. Cases of SOD1 mutations had the most extensive mislocalization in both astrocytic nucleus and neuronal nucleus. Cases of wild-type cells with wt-SOD1 had definitely not mislocalization but normal colocalization and normal shaped nucleus as a consistent feature (Fig 3A, Fig. 5). A case of wild-type cells with the G93A-SOD1 mutation, with a known display of substantial cytoplasmic SOD1 localization and negative for SOD1 pathology, revealed an intermediate amount of misfolded SOD1 accumulation and mislocalization in the primary astrocytic cells and neuronal cells. We further used mutant G93A-SOD1 to demonstrate immunoreactivity for mislocalized SOD1 in astrocytes and mutant neurons by transfection and increased ratio of mislocalization of nucleus in both astrocytes and neurons.

Accumulation of wild-type and mutant SOD1 in detergent-insoluble aggregates in neurons and astrocytes expressing mutant SOD1

In studies of cortical neurons and astrocytes, we have viewed wt SOD1 as being relatively resistant to aggregation. Here, we also evaluated the ability of G93A-SOD1 to modulate the aggregation of not only mutant G93A-SOD1 but also wt SOD1 in cortical cell culture. At 48 h after transfection, we observed significant accumulation of aggregated SOD1 proteins in cells transfected with mutant G93A-SOD1. The intra-cytoplasmic localization of aggregates containing G93A-SOD1 immunoreactivity is clearly demonstrated in fluorescence images (Fig. 6A). By estimating, in each single cell, the ratio between wtSOD1 transfected cells and mutant G93A-SOD1 transfected cells, we found a robust increase of the intra-cytoplasmic G93A-SOD1 protein with respect to the wtSOD1. However, in cells wt transfected with wtSOD1, aggregate forms were virtually lower detectable(Fig. 6B). This finding indicates that the higher levels of the G93A-SOD1 aggregates in wild-type cortical astrocytes modulate the generation of these aggregates.

Expression of both wtSOD1 and mutant SOD1 in neurons and astrocytes trigger cell death by transfection mutant SOD1

In preparations of nuclei, we also analyzed the presence of SOD1 immunoreactivity in comparison with DAPI staining. The results indicate that the wt SOD1 immunoreactivity colocalizes with DAPI staining, whereas the G93A-SOD1 immunoreactivity rarely does, thus confirming

that the nuclei of cells expressing the mutant SOD1 do not contain the enzyme (Fig. 6A). The exclusion of the mutant SOD1 from the nuclei may be due either to the formation of high MW species, unable to diffuse through the nuclear membrane, or to an increased nuclear degradation of the aberrant protein. In the second case, the G93A-SOD1 misfolding may be exacerbated by the nuclear environment, leading to a faster degradation by G93A-SOD1 transfection (Fig. 6B). The results presented so far indicate that SOD1 may remove free radical species not only in the cytoplasm, where it is mainly located, but also in the nucleus. In this latter compartment, wtSOD1 may serve to protect from protein oxidation and DNA mutations caused by oxidative stress. We thus investigated whether the generation of free radical species may increase nuclear damage in cortical neurons and astrocytes expressing G93A-SOD1 by transfection (Fig. 7A, B). The results show that our cell culture studies indicate that WT protein can modulate the aggregation of mutant SOD1 and it is thus tempting to suggest that one mechanism by which WT SOD1 accelerates the course of cell death is by transfection with mutant G93A-SOD1 to produce toxic species.

Cytoplasmic accumulation of protein aggregates in primary astrocytes promote apoptosis

Compared to cells with wild-type SOD1, the number of cleaved-Caspase-3 positive cells is strongly increased in mutant cells with mutant G93A-SOD1 (Fig. 8C) suggesting that activation of apoptosis is at least

dependent on the G93A-SOD1 (Fig. 8A, B). Importantly, however, these results demonstrates that the cleaved caspase-3 antibody still detect wt astrocytes with G93A-SOD1 and wt neurons with G93A-SOD1 (not shown). The cleaved caspase-3 antibody specifically detects the cortical neurons and astrocytes with G93A-SOD1 in apoptotic cells. Thus, we proposed that mutant G93A-SOD1 mediates toxic events in apoptosis, with large detergent-insoluble aggregates playing roles in wt SOD1 transformed to G93A-SOD1 forms of the protein involved in events that initiate disease. Collectively, these results indicated that the wt SOD1 plays some role in modulating the toxicity of G93A-SOD1 which involved in aggregates and mislocalization of nucleus in cells with G93A-SOD1.

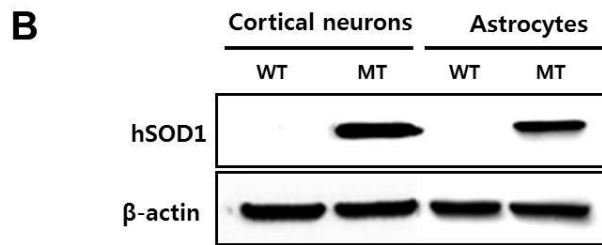
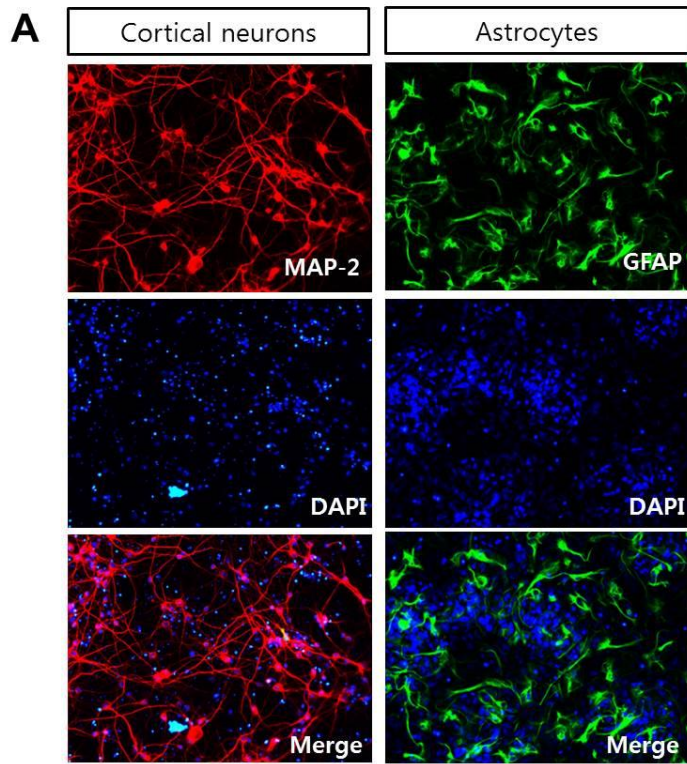


Figure 1. Cellular and morphological characterization of astrocyte and neuron enriched cultures

(A) Immunofluorescent staining for MAP-2 of cortical neurons (red), for GFAP (green) of astrocytes with DAPI for nuclei (blue). (B) Western blot analysis confirmed the presence of the human SOD1 in cortical neurons and astrocytes. Representative western blot probed for hSOD1 and β -actin simultaneously. Levels of hSOD1 in both mutant cortical neurons and mutant astrocytes increased compared with wild-type.

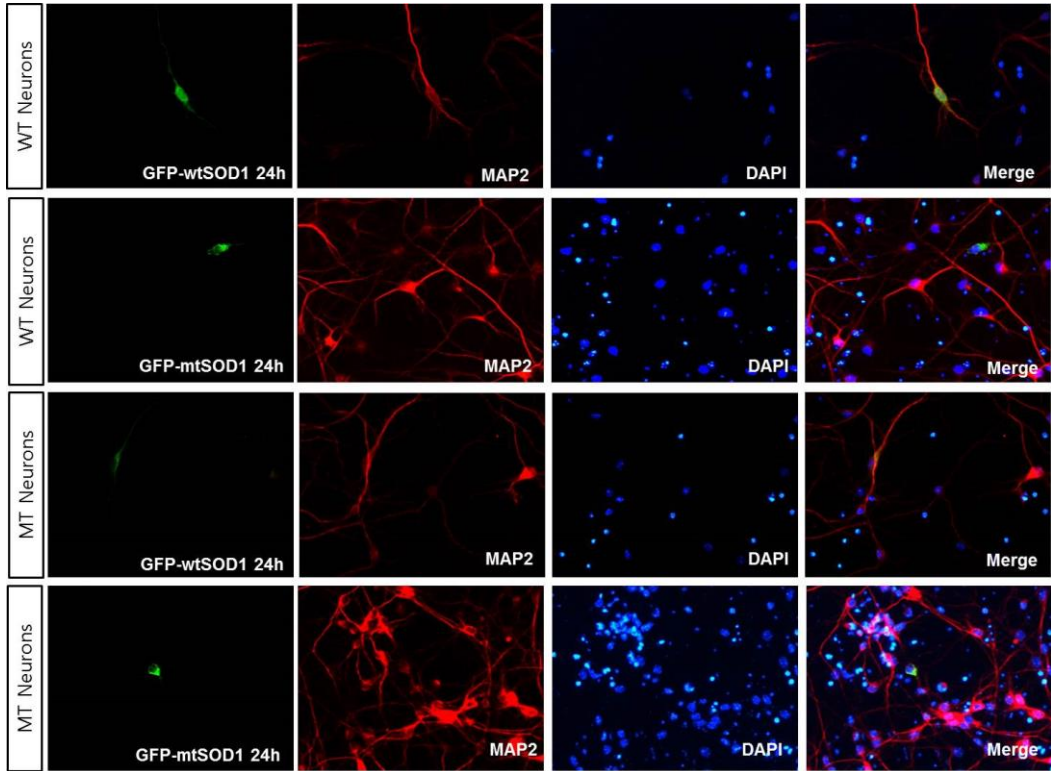
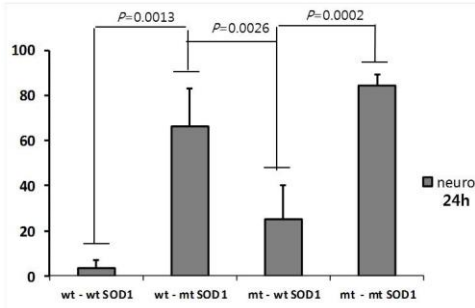


Figure 2. Wild-type neuronal cells transformed mutant form by transfection G93A-SOD1

Primary cortical neurons stained against MAP-2 (red) and DAPI (blue) nuclear counterstain. Wild-type SOD1 predominantly colocalizes in the nucleus while transfected with the mutant G93A-SOD1 localizes in the cytosol.

A Neuron_Mislocalization



B Neuron_Cell death

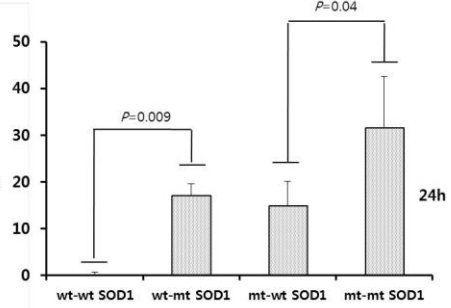


Figure 3. Wild-type neuronal cells transformed mutant form by transfection G93A-SOD1

Cortical neurons were transfected with wild-type (WT) SOD1 and mutant G93A-SOD1, and mislocalization and cell death were examined by DAPI staining. In the wild-type cortical neurons with mutant G93A-SOD1 transfectant increased mislocalization and cell death.

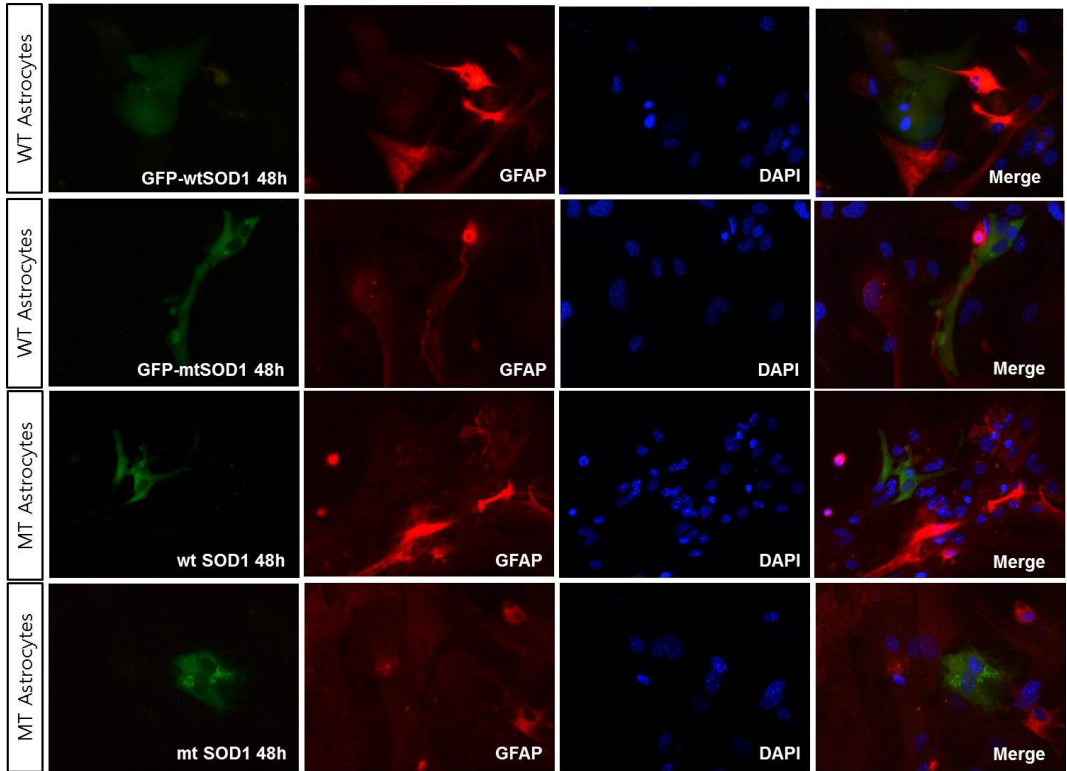


Figure 4. Wild-type and mutant astrocytes transformed mutant form by transfection GFP-wild type and G93A-SOD1

Astrocytes stained against GFAP (red) and DAPI (blue) nuclear counterstain. Wild-type astrocytes with wild-type hSOD1-GFP transfectants predominantly colocalizes in the cytoplasm and nucleus while transfected with the mutant G93A-SOD1 localizes in the cytosol.

Astrocyte_Mislocalization

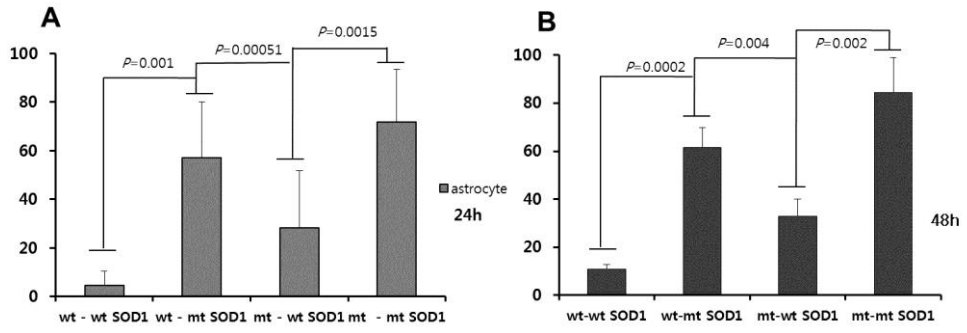


Figure 5. Cytoplasmic mislocalization in the wild-type and mutant astrocytes by transfection GFP-wild type and G93A-SOD1

Astrocytes were transfected with wild-type SOD1 and mutant G93A-SOD1. Cytoplasmic mislocalization was examined by the presence of the hSOD1-EGFP fluorescence at 24h and 48h post-transfection.

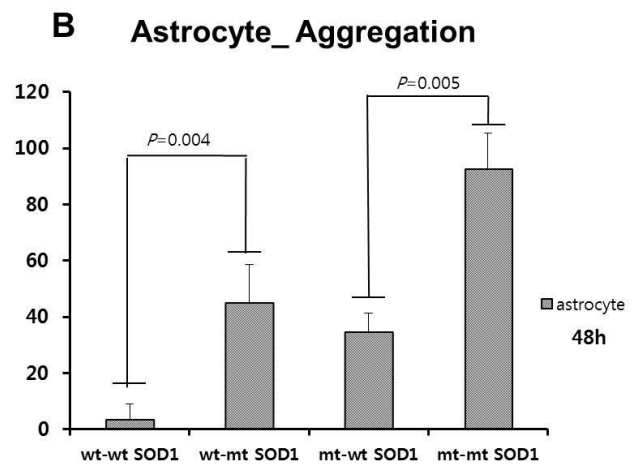
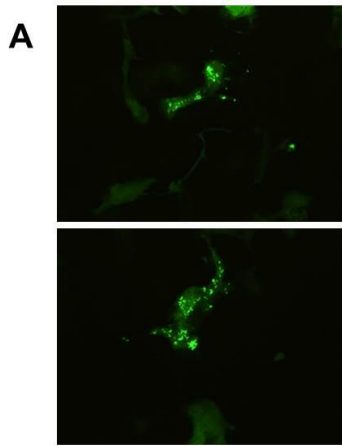


Figure 6. Aggregated formation of mutant SOD1 in mutated astrocytes by transfection GFP-mutant SOD1

(A) Intracellular aggregates of astrocytes were induced by incubation with transfected G93A-SOD1. (B) Aggregate formation was examined by the presence of the hSOD1-EGFP fluorescence in the cytoplasmic area at 48h post-transfection.

Astrocyte_Cell death

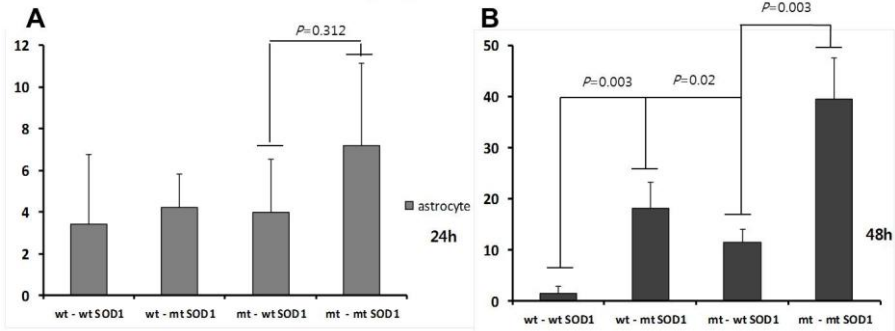


Figure 7. Expression of both wt-SOD1 and mt-SOD1 induces cell death by transfection mutant SOD1 in astrocytes

Astrocytes were transfected with wild-type and mutant G93A-SOD1, and cell death was examined by DAPI staining. In the wild-type astrocytes with mutant G93A-SOD1 transfectant increased cell death. Expression of mutant G93A-SOD1 significantly increased apoptotic cell death in astrocytes induced by transfection.

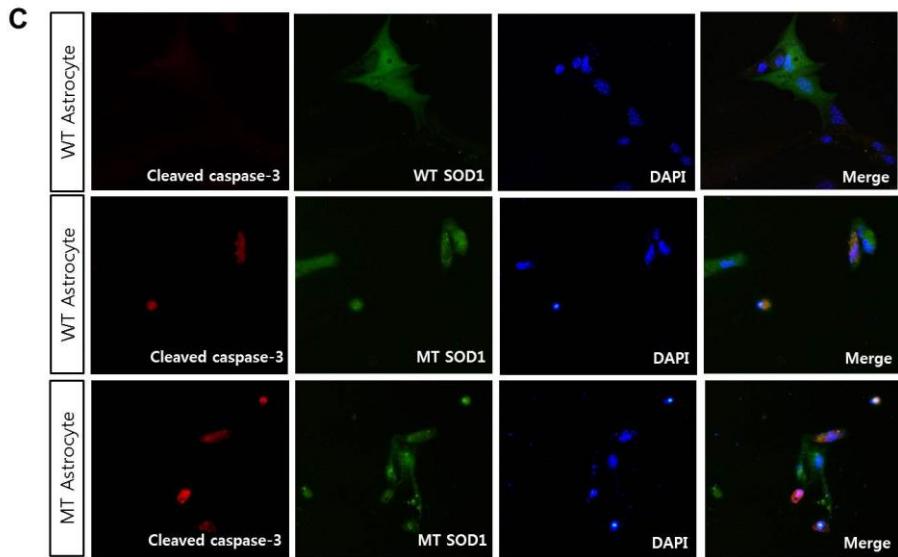
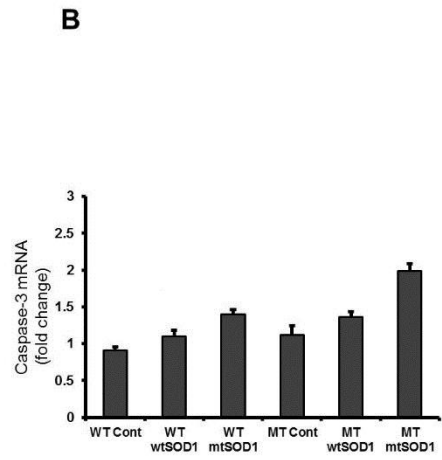
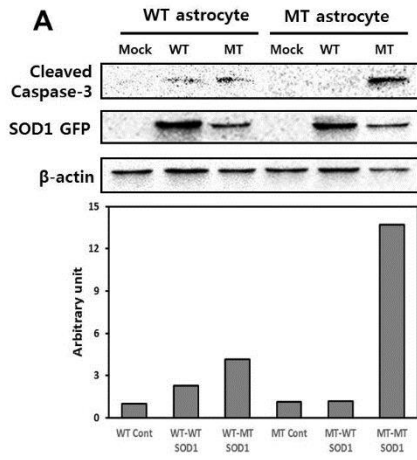


Figure 8. Cytoplasmic accumulation of protein aggregates in primary astrocytes promote apoptosis

(A) Expression of cleaved caspase-3 protein was largely increased in mutant G93A-SOD1 transfected astrocytes. By contrast, expression of cleaved caspase-3 was not affected in the wild-type astrocytes with wild-type SOD1 transfectants.

(B) Real-time quantitative PCR analysis of caspase-3 mRNA. Interestingly, we detected a increase in the expression of caspase-3 mRNA in mutant G93A-SOD1 transfected astrocytes. Immunofluorescent staining on primary astrocytes for cleaved caspase-3 (red) and the nuclear stain DAPI (blue). Wild-type and mutant hSOD1-EGFP transfectants (green).

IV. Discussion

SOD1 loss of function was initially thought to play a role in ALS due to the discovery of disease-causing mutations in the SOD1 gene and due to the well-established link between oxidative stress and neurodegeneration (Smith et al., 1991; Stadtman, 1992; Stadtman and Berlett, 1997). As SOD1-familial ALS undoubtedly arises primarily from SOD1 toxic gain of function, the loss of chronic oxidative stress.

The data here presented indicate that, in the nucleus of both cortical neurons and astrocytes of transgenic mice embryos expressing either human wtSOD1 or mutant G93A-SOD1, the level of mutant SOD1 are reduced compared with those of wtSOD1. This may be because of the formation of insoluble high MW species of mutant G93A-SOD1 that prevent the diffusion of the protein across the nuclear membrane, whereas this diffusion is possible for wtSOD1. An alternative possibility is that mutant G93A-SOD1 nuclear deprivation might be because of its faster turnover in this compartment when compared with wtSOD1. Reduced levels of G93A-SOD1 may reflect a decrease of its enzymatic activity and, thus, a decreased removal of free radical species inside the nucleus. The obvious consequence of the loss of this protective function of SOD1 in the nucleus is that genomic DNA may be more easily altered by the attack of reactive species; this, in turn, may induce cell death, and consequently, alterations in the protein expression profile in cortical

neurons and astrocytes.

SOD1 activity is generally reduced to approximately half of normal in patients with SOD1-familial ALS, owing to reduced SOD1 messenger RNA half-life in the CNS and due to possible effects of SOD1 protein misfolding and aggregation on activity. Our findings indicate that the effect of wtSOD1 on the toxicity of mutant G93A-SOD1 is influenced by both the fALS mutation cortical neurons and astrocytes with expressed mutant SOD1. From cell culture models of aggregation, we find that wtSOD1 modulates the aggregation of the mutant protein to the formation of large detergent-insoluble structures. In wt cells with G93A-SOD1, the aggregation of the mutant and WT proteins confounds determination of whether the presence of the WT SOD1 changes the mutant form. Together, these findings implicate soluble assemblies of wt and mutant G93A-SOD1 as possible mediators of toxic processes involved in initiating mislocalization and aggregates. We used immortalized cortical neurons and astrocytes that reasonable to assume that the mechanism we describe is relevant in cortical neurons and astrocytes because of both similar effects in fALS. Further, the results indicated that only cortical neurons have selective vulnerability in cell death by transfection with G93A-SOD1. Thus, in cortical neurons and astrocytes expressing wt SOD1 with G93A-SOD1 by transfection, it is clear that the magnitude of the effect of wt SOD1 on the toxicity of mutant SOD1 is related to the level of mutant SOD1 expression. Clearly, the toxicity of these mutants is dramatically augmented by the transfection of G93A-SOD1. These observations suggest that mutant

G93A-SOD1 is probably interacting with wt SOD1 via some mechanisms to produce the augmented toxicity.

The conformational conversion of natively structured SOD1 is analogous to the conversion of the natively folded prion protein (PrP^C) to a misfolded conformer of the same protein (PrP^{Sc}) in prion disease. Two mechanisms have been proposed to account for the PrP^C→PrP^{Sc} conversion process: nucleation-polymerization, in which the misfolded monomeric PrP^{Sc} is intrinsically less stable as a monomer but becomes more stable than PrP^C when recruited to a multimolecular PrP^{Sc} aggregate; and template mediated assistance, in which the PrP^{Sc} conformer is more stable than PrP^C but kinetically inaccessible without catalysis by interaction with PrP^{Sc} (Horwich and Weissman, 2010). Seeded polymerization of proteins can be regarded as recruitment of partially unfolded molecular species to an aggregate, whereas in template assistance, partially unfolded recruitable intermediates are first generated by contact between natively folded molecular species and the template. Further study is needed to understand how the SOD1 misfolding mechanism can be placed in this conceptual framework, but one may speculate from the evidence above that the misfolding mechanisms of mutant SOD1 and wtSOD1 span a continuum from seeded polymerization to template assistance. Aggregation of partially unfolded mutant SOD1 may propagate primarily by seeded polymerization, whereas conversion of wtSOD1 may necessitate structural loosening induced by contact with a mutant the misfolded SDO1 seed. In support of this notion is the recent finding that wtSOD1 can only participate in

seeded polymerization on exposure to low pH and the chaotrope guanidine *in vitro* (Bosco et al., 2010), conditions that destabilize the native state and favor seeded polymerization.

SOD1 has a crucial role in superoxide clearance and its loss of function generates an increased state of oxidative stress. In a tgSOD1-ALS mouse model, SOD1 is itself a major target of oxidization (Andrus et al., 1998) and SOD1 oxidation and glutathionylation, which occurs in response to oxidative stress, both increase the propensity of the dimer to dissociate and become misfolded (Khare et al., 2004; Rakhit et al., 2004; Ezzi et al., 2007; Wilcox et al., 2009). Indeed, the oxidized SOD1 has an increased propensity to misfold, causing seeding and aggregation of SOD1 and resulting in a reduction of dismutase activity. We note that the strong link between SOD1 misfolding and its mislocalization make the two effects very difficult to assess independently. Recent studies demonstrating that SOD1 aggregation can be seeded *in vitro* from mouse tg G93A-SOD1 spinal cord material (Chia et al., 2010), and 'transmitted' between cells (Munch et al., 2011) extend the potential role for these pathogenic mechanisms to the clinical and pathological 'spread' of ALS (Ravits et al., 2007; Pokrishevsky et al., 2012). Of note, SOD1 was also found to be oxidized in Alzheimer's disease and Parkinson's disease (Choi et al., 2005).

Results reported in this paper further strengthen the hypothesis that mutant G93A-SOD1 modulates the mislocalization and aggregation in ALS-associated SOD1 in cortical neurons and astrocytes that through

wtSOD1 transformed mutant form by transfected with G93A-SOD1. In conclusion, in this work we provide a new model for a cellular network mutant G93A-SOD1 with wtSOD1 interactions from G93A-SOD1-induced cell death.

V. References

1. Acevedo-Arozena A, Kalmar B, Essa S, Ricketts T, Joyce P, Kent R, et al. A comprehensive assessment of the SOD1G93A low-copy transgenic mouse, which models human amyotrophic lateral sclerosis. *Dis Model Mech* 2011; 4: 686-700.
2. Andersen PM, Al Chalabi A. Clinical genetics of amyotrophic lateral sclerosis; what do we really know? *Nat Rev Neurol* 2011; 7: 603-15.
3. Andrus PK, Fleck TJ, Gurney ME, Hall ED. Protein oxidative damage in a transgenic mouse model of familial amyotrophic lateral sclerosis. *J Neurochem* 1998; 71: 2041-8.
4. Basso M, Massignan T, Samengo G, Cheroni C, De Biasi S, Salmona M, Bendotti C, Bonetto V. *J BiolChem* 2006; 281: 33325-33335.
5. Beghi E, Mennini T, Bendotti C, Bigini P, Logroscino G, Chio A, et al. The heterogeneity of amyotrophic lateral sclerosis: a possible explanation of treatment failure, *Curr Med Chem* 2007; 14: 3185-200.
6. Bendotti, C and Carri, M.T. Lessons from models of SOD1-linked familial ALS. *Trends Mol. Med* 2004; 10: 393-400.
7. Boillee, S., VandeVelde, C. and Cleveland, D.W. ALS: a disease of motor neurons and their nonneuronal neighbors. *Neuron* 2006;

52: 39-59.

8. Bosco DA, et al. Wild-type and mutant SOD1 share an aberrant conformation and a common pathogenic pathway in ALS. *Nat Neurosci* 2010; 13: 1396-1403.
9. Cashman NR, Durham HD, Blusztajn JK, Oda K, Tabira T, Shaw IT, Dahrouge S, Antel JP. Neuroblastoma x spinal cord (NSC) hybrid cell lines resemble developing motor neurons. *Dev Dyn* 1992; 194: 209-221.
10. Chang LY, Slot JW, Geuze HJ, Crapo JD. Molecular immunocytochemistry of the CuZn superoxide dismutase in rat hepatocytes. *J Cell Biol* 1988; 107: 2169-79.
11. Chattopadhyay M, Durazo A, Sohn SH, Strong CD, Gralla EB, Whitelegge JP, Valentine JS. Initiation and elongation in fibrillation of ALS-linked superoxide dismutase. *Proc Natl Acad Sci USA* 2008; 105: 18663-18668.
12. Chia R, Tattum MH, Jones S, Collinge J, Fisher EM, Jackson GS. Superoxide dismutase 1 and tgSOD1 mouse spinal cord seed fibrils, suggesting a propagative cell death mechanism in amyotrophic lateral sclerosis. *PLoS One* 2010; 5: e10627.
13. Choi J, Rees HD, Weintraub ST, Levey AI, Chin LS, Li L. Oxidative modifications and aggregation of Cu,Zn-superoxide dismutase associated with Alzheimer and Parkinson diseases. *J Biol Chem* 2005; 280: 11648-55.

14. Crapo JD, Oury T, Rabouille C, Slot JW, Chang LY. Copper,zinc superoxide dismutase is primarily a cytosolic protein in human cells. *ProcNatlAcadSci USA* 1992; 89: 10405-9.
15. Deng HX, Hentati A, Tainer JA, Iqbal Z, Cayabyab A, Hung WY, et al. Amyotrophic lateral sclerosis and structural defects in Cu,Zn superoxide dismutase. *Science* 1993; 261: 1047-51.
16. Deng HX, Jiang H, Fu R, Zhai H, Shi Y, Liu E, Hirano M, Dal Canto MC, Siddique T. Molecular dissection of ALS-associated toxicity of SOD1 in transgenic mice using an exon-fusion approach. *Hum Mol Genet* 2008; 17: 2310-2319.
17. Deng HX, Shi Y, Furukawa Y, Zhai H, Fu R, Liu E, Gorrie GH, Khan MS, Hung WY, Bigio EH, et al. Conversion to the amyotrophic lateral sclerosis phenotype is associated with intermolecular linked insoluble aggregates of SOD1 in mitochondria. *ProcNatlAcadSci USA* 2006; 103: 7142-7147.
18. Dugan LL, Kim-Han JS. Astrocyte mitochondria in in vitro models of ischemia. *J BioenergBiomembr* 2004; 36: 317-321.
19. Durham HD, Dahrouge S, Cashman NR. Evaluation of the spinal cord neuron x neuroblastoma hybrid cell line NSC34 as a model for neurotoxicity testing. *Neurotoxicology* 1992; 14: 387-395.
20. Ezzi SA, Urushitani M, Julien JP, Wild-type superoxide dismutase acquires binding and toxic properties of ALS-linked mutant forms through oxidation. *J Neurochem* 2007; 102: 170-8.

21. Fridovich I. Superoxide radical and superoxide dismutases. *Annu Rev Biochem* 1995; 64: 97-112.
22. Greenamyre JT, Betarbet R, Sherer TB. The rotenone model of Parkinson's disease: genes, environment and mitochondria. *Parkinsonism RelatDisord* 2003; 9: S59-S64.
23. Gurney ME, Pu H, Chiu AY, Dal Canto MC, Polchow CY, Alexander DD, Caliendo J, Hentati A, Kwon YW, Deng HX, et al. Motor neuron degeneration in mice that express a human Cu,Zn superoxide dismutase mutation. *Science* 1994; 264: 1772-1775.
24. Horwich AL, Weissman JS. Deadly conformations-protein misfolding in prion disease. *Cell* 1997; 89: 499-510.
25. Jonsson PA, Graffmo KS, Andersen PM, Brannstrom T, Lindberg M, Oliveberg M, Marklund SL. Disulphide-reduced superoxide dismutase-1 in CNS of transgenic amyotrophic lateral sclerosis models. *Brain* 2006; 129: 451-464.
26. Karch Cm, Prudencio M, Winkler DD, Hart PJ, Borchelt DR. Role of mutant SOD1 disulfide oxidation and aggregation in the pathogenesis of familial ALS. *ProcNatlAcadSci USA* 2009; 106: 7774-7779.
27. Keller GA, Warner TG, Steimer KS, Hallewell RA. Cu,Zn superoxide dismutase is a peroxisomal enzyme in human fibroblasts and hepatoma cells. *ProcNatlAcadSci USA* 1991; 88: n7381-5.

28. Khare SD, Caplow M, Dokholyan NV. The rate and equilibrium constants for a multistep reaction sequence for the aggregation of superoxide dismutase in amyotrophic lateral sclerosis. *ProcNatlAcadSci USA* 2004; 101: 15094-9.
29. Munch C, O'Brien J, Bertolotti A. Prion-like propagation of mutant superoxide dismutase-1 misfolding in neuronal cells. *ProcNatlAcadSci USA* 2011; 108: 3548-53.
30. Pasinelli P, Brown RH. Molecular biology of amyotrophic lateral sclerosis: insights from genetics. *Nat Rev Neurosci* 2006; 7: 710-23.
31. Pokrishevsky E, Grad LI, Yousefi M, Wang J, Mackenzie IR, Cashman NR. Aberrant localization of FUS and TDP43 is associated with misfolding of SOD1 in amyotrophic lateral sclerosis. *PLoS One* 2012; 7: e35050.
32. Prudencio M, Durazo A, Whitelegge JP, Borchelt DR. Modulation of mutant superoxide dismutase 1 aggregation by co-expression of wild-type enzyme. *J Neurochem* 2009; 108: 1009-1018.
33. Prudencio M, Hart PJ, Borchelt DR, Andersen PM. Variation in aggregation propensities among ALS-associated variants of SOD1: correlation to human disease. *Hum Mol Genet* 2009; 18: 3217-3226.
34. Rakhit R, Crow JP, Lepock JR, Kondejewski LH, Cashman NR, Chakrabartty A. Monomeric Cu,Zn-superoxide dismutase is a

common misfolding intermediate in the oxidation models of sporadic and familial amyotrophic lateral sclerosis. *J BiolChem* 2004; 279: 15499-504.

35. Ravits J, Laurie P, Fan Y, Moore DH. Implications of ALS focality: rostral-caudal distribution of lower motor neuron loss postmortem. *Neurology* 2007; 68: 1576-82.
36. Reddi AR, Culotta VC. SOD1 integrates signals from oxygen and glucose to repress respiration. *Cell* 2013; 152: 224-35.
37. Rosen DR, Siddique T, Patterson D, Figlewicz DA, Sapp P, Hentati A, et al. Mutations in Cu/Zn superoxide dismutase gene are associated with familial amyotrophic lateral sclerosis. *Nature* 1993; 362: 59-62.
38. Shefner JM, Reaume AG, Flood DG, Scott RW, Kowall NW, Ferrante RJ, Siwek DF, Upton-Rice M and Brown RH Jr. Mice lacking cytosolic copper/zinc superoxide dismutase display a distinctive motor axonopathy. *Neurology* 1999; 53: 1239-1246.
39. Smith CD, Carney JM, Starke-Reed PE, Oliver CN, Stadtman ER, Floyd RA, et al. Excess brain protein oxidation and enzyme dysfunction in normal aging and in Alzheimer disease. *ProcNatlAcadSci USA* 1991; 88: 10540-3.
40. Sofroniew MV, Vinters HV. Astrocyte: biology and pathology. *ActaNeuropathol* 2010; 119: 7-35.

41. Stadtman ER. Protein oxidation and aging. *Science* 1992; 257: 1220-4.
42. Stadtman ER, Berlett BS. Reactive oxygen-mediated protein oxidation in aging and disease. *Chem Res Toxicol* 1997; 10: 485-94.
43. Sturtz LA, Diekert K, Jensen LT, Lill R, Culotta VC. A fraction of yeast Cu, Zn-superoxide dismutase and its metallochaperone, CCS, localize to the intermembrane space of mitochondria. A physiological role for SOD1 in guarding against mitochondrial oxidative damage. *J BiolChem* 2001; 276: 38084-9.
44. Wang J, Slunt H, Gonzales V, Fromholt D, Coonfield M, Copeland NG, Jenkins NA, Borchelt DR. Copper-binding-site-null SOD1 causes ALS in transgenic mice: aggregates of non-native SOD1 delineate a common feature. *Hum Mol Genet* 2003; 12: 2753-2764.
45. Wang L, Deng HX, Grisotti G, Zhai H, Siddique T, Roos RP. Wild-type SOD1 overexpression accelerates disease onset of a G85R SOD1 mouse. *Hum Mol Genet* 2009; 18: 1642-1651.
46. Wang Q, Johnson JL, Agar NY, Agar JN. Protein aggregation and protein instability govern familial amyotrophic lateral sclerosis patient survival. *PLoS Biol* 2008; 76: e170.
47. Wilcox KC, Zhou L, Jordon JK, Huang Y, Yu Y, Redler RL, et al. Modifications of superoxide dismutase (SOD1) in human

erythrocytes: a possible role in amyotrophic lateral sclerosis. *J BiolChem* 2009; 284: 13940-7.

48. Witan H, Gorlovoy P, Kaya AM, Koziollek-Drechsler I, Neumann H, Behl C, Clement AM. Wild-type Cu/Zn superoxide dismutase (SOD1) does not facilitate, but impedes the formation of protein aggregates of amyotrophic lateral sclerosis causing mutant SOD1. *Neurobiol Dis* 2009; 36: 331-342.

국문초록

근위축성측삭경화증 (Amyotrophic lateral sclerosis, ALS)은 상위 운동신경세포와 하위운동신경세포의 선택적 손상으로 사지의 위축이 서서히 진행되고, 결국에는 호흡근 마비로 수년 내에 사망하게 되는 치명적인 질환이다. 대부분의 경우는 산발성이나 전체의 10%는 가족성으로 발병하며 그 중의 20%에서는 SOD1 (superoxide dismutase)의 유전자 돌연변이 현상으로 인한 기전으로 알려져 있다.

최근 연구 동향은 ALS에서 운동신경세포가 손상받는 여러 기전 중 SOD1의 돌연변이에 의한 비정상적인 단백질의 응집 및 성상아교세포의 독성효과가 중요하게 작용할 것으로 생각되고 있다. 이에 본 연구에서는 ALS 발병기전에서 신경세포 및 성상아교세포에서 비정상적인 단백질의 응집을 유발하여 일련의 세포내 변화를 연구하기 위하여 기획하였다.

연구 방법으로 G93A-SOD1의 돌연변이 쥐에서 임신 후 16일째의 wild-type과 G93A 돌연변이 배아들을 분리, 초대배양하여 이를 각 신경세포와 성상아교세포로 분화시켰다. 이후 wild-type SOD1 유전자와 G93A-SOD1의 돌연변이 유전자를 각 세포에 트랜스펙션하여 세포의 특징적인 변화를 관찰한 후 결과를 비교분석하여 아래와 같은 결과를 얻었다.

1. Wild-type의 신경세포와 성상아교세포에 G93A-SOD1 돌연변이 유전자를 트랜스펙션하면 신경세포와 성상아교세포가 돌연변이 유전자

를 발현하는 세포의 특징을 나타낸다.

2. G93A-SOD1 돌연변이 유전자를 발현하는 신경세포와 성상아교세포에서는 wild-type SOD1 과 돌연변이 SOD1 유전자로 인해 세포에 비정상적인 단백질의 응집현상이 일어난다.

3. G93A-SOD1 돌연변이 유전자를 트랜스펙션하면 G93A-SOD1을 발현하는 세포뿐만 아니라 wild-type SOD1을 발현하는 세포에서도 세포사멸이 유도된다.

4. G93A-SOD1 돌연변이 유전자를 발현하는 신경세포와 성상아교세포에서 wild-type SOD1과 돌연변이 SOD1 유전자로 인해 세포에 응집현상이 일어나면 세포사멸을 유도하게 되고 신경아교세포에 비해 신경세포가 SOD1의 독성효과에 더욱 취약함을 보여준다.

이상의 연구결과에 기준하여 연구자는 G93A-SOD1 돌연변이 유전자는 wild-type SOD1과 비교하여 세포응집과 이에 따른 세포사멸 현상이 뚜렷하였으며, 이는 향후 근위축성측삭경화증에서 SOD1의 유전자 돌연변이 현상으로 인한 기전 및 발병기전을 규명하고 나아가 치료방법을 개발하는데 중요한 단서를 제공할 것으로 사료된다.